Neurochemistry International 143 (2021) 104935

Contents lists available at ScienceDirect

Neurochemistry International

journal homepage: www.elsevier.com/locate/neuint

Accumbal D2R-medium spiny neurons regulate aversive behaviors through PKA-Rap1 pathway

You-Hsin Lin [a], Yukie Yamahashi [b], Keisuke Kuroda [a], Md. Omar Faruk [a], Xinjian Zhang [c], Kiyofumi Yamada [d], Akihiro Yamanaka [e], Taku Nagai [c,**], Kozo Kaibuchi [a,b,*]

[a] Department of Cell Pharmacology, Graduate School of Medicine, Nagoya University, Nagoya, Aichi, 466-8550, Japan
[b] Institute for Comprehensive Medical Science, Fujita Health University, Toyoake, Aichi, 470-1129, Japan
[c] Division of Behavioral Neuropharmacology, Project Office for Neuropsychological Research Center, Fujita Health University, Toyoake, Aichi, 470-1129, Japan
[d] Department of Neuropsychopharmacology and Hospital Pharmacy, Graduate School of Medicine, Nagoya University, Nagoya, Aichi, 466-8550, Japan
[e] Department of Neuroscience II, Research Institute of Environmental Medicine, Nagoya University, Nagoya, Aichi, 464-8601, Japan

ARTICLE INFO

Keywords:
Adenosine
Medium spiny neuron
Mental health
Nucleus accumbens
PKA

ABSTRACT

The nucleus accumbens (NAc) plays a crucial role in various mental activities, including positive and negative reinforcement. We previously hypothesized that a balance between dopamine (DA) and adenosine signals regulates the PKA-Rap1 pathway in medium spiny neurons expressing DA D1 receptors (D1R-MSNs) or D2 receptors (D2R-MSNs) and demonstrated that the PKA-Rap1 pathway in D1R-MSNs is responsible for positive reinforcement. Here, we show the role of the PKA-Rap1 pathway in accumbal D2R-MSNs in negative reinforcement. Mice were exposed to electric foot shock as an aversive stimulus. We monitored the phosphorylation level of Rap1gap S563, which leads to the activation of Rap1. Electric foot shocks increased the phosphorylation level of GluN1 S897 and Rap1gap S563 in the NAc. The aversive stimulus-evoked phosphorylation of Rap1gap S563 was detected in accumbal D2R-MSNs and inhibited by pretreatment with adenosine A2a receptor (A2aR) antagonist. A2aR antagonist-treated mice showed impaired aversive memory in passive avoidance tests. AAV-mediated inhibition of PKA, Rap1, or MEK1 in accumbal D2R-MSNs impaired aversive memory in passive avoidance tests, whereas activation of this pathway potentiated aversive memory. Optogenetic inactivation of mesolimbic DAergic neurons induced place aversion in real-time place aversion tests. Aversive response was attenuated by inhibition of PKA-Rap1 signaling in accumbal D2R-MSNs. These results suggested that accumbal D2R-MSNs regulate aversive behaviors through the A2aR-PKA-Rap1-MEK pathway. Our findings provide a novel molecular mechanism for regulating negative reinforcement.

1. Introduction

Nucleus accumbens (NAc) plays a pivotal role in various mental activities, including positive and negative reinforcement (Hu 2016). Approximately 95% of the neurons in NAc are medium spiny neurons (MSNs), which are subdivided into dopamine (DA) D1 receptor (D1R)-expressing MSNs (D1R-MSNs) and DA D2 receptor (D2R)-expressing MSNs (D2R-MSNs) (Surmeier et al., 2007; Smith et al., 2013). D1R-MSNs and D2R-MSNs are thought to be involved in positive reinforcement and negative reinforcement, respectively (Bromberg-Martin et al., 2010; Ferguson et al., 2011; Kravitz et al., 2012; Lobo et al., 2013). The functional segregation of D1R-MSNs and D2R-MSNs primarily depends on various neuromodulators and neurotransmitters, including DA and adenosine in the NAc (Nakanishi et al., 2014).

It is well-known that striatal DA-D1R-protein kinase A (PKA) signaling regulates reward-related behavior (Cepeda et al., 1993; Surmeier et al., 1995). When extracellular DA increases after reward acquirement or abused drug intake, D1R stimulation leads to the activation of PKA and its downstream substrates through D1R coupling to G_{olf} proteins. We previously carried out a phosphoproteomic analysis to explore D1R downstream PKA substrates and found more than 100 PKA substrate candidates, including Rasgrp2 and Rap1gap (Nagai et al.,

* Corresponding author. Department of Cell Pharmacology, Graduate School of Medicine, Nagoya University, Nagoya, Aichi, 466-8550, Japan.
** Corresponding author. Division of Behavioral Neuropharmacology, Project Office for Neuropsychological Research Center, Fujita Health University, 1-98 Dengakugakubo, Kutsukake-cho, Toyoake, Aichi, 470-1192, Japan.
E-mail addresses: taku.nagai@fujita-hu.ac.jp (T. Nagai), kaibuchi@med.nagoya-u.ac.jp (K. Kaibuchi).

https://doi.org/10.1016/j.neuint.2020.104935
Received 17 September 2020; Received in revised form 19 November 2020; Accepted 4 December 2020
Available online 7 December 2020

2016a). Rasgrp2 is a guanine nucleotide exchange factor (GEF) for small GTPase Rap1; PKA-mediated phosphorylation of Rasgrp2 at S116, S117, S554, and S586 leads to Rap1 activation (Nagai et al., 2016a). Rap1gap is a GTPase-activating protein (GAP) and negatively regulates Rap1. PKA-mediated phosphorylation of Rap1gap S563 has been shown to inactivate GAP activity on Rap1 and lead to Rap1 activation (McAvoy et al., 2009; Zhang et al., 2019). PKA efficiently promotes Rap1 activation through Rasgrp2 and Rap1gap phosphorylation. Rap1 activation increases the excitability of accumbal D1R-MSNs through MEK1-MAPK and eventually induces reward-related behaviors (Nagai et al., 2016a).

PKA-Rap1 signaling is also found in D2R-MSNs and regulated by D2R and adenosine A2a receptors (A2aR) (Zhang et al., 2019). D2R is a Gi-coupled receptor and has a high affinity for DA compared with D1R. Therefore, PKA signaling transmission is suppressed under basal DA concentration (Nair et al., 2015). A2aR is exclusively expressed on D2R-MSNs in the NAc, and stimulation of A2aR promotes PKA signaling pathway through G_{olf} protein (Fink et al., 1992; O'Neill et al., 2012; Svenningsson et al., 1999). We have demonstrated that D2R inhibition or A2aR stimulation promotes Rap1 activation through Rap1gap phosphorylation in D2R-MSNs of NAc (Zhang et al., 2019).

Aversive stimuli, including pinch, air puff, and electric shock, are known to modulate the activity of DAergic neurons (McCutcheon et al., 2012; Badrinarayan et al., 2012). Electric foot shock has been shown to decrease the amount of DA in the NAc (de Jong et al., 2019) and activate PKA signaling in D2R-MSNs (Yamaguchi et al., 2015). However, the role of the PKA-Rap1 pathway in negative reinforcement remains unknown in accumbal D2R-MSNs.

In this study, we aimed to clarify how adenosine-A2aR signaling in D2R-MSN regulates negative reinforcement. We monitored the phosphorylation level of Rap1gap S563 and the effect of A2aR antagonist on Rap1gap phosphorylation after electric foot shock aversive stimulus. We also examined the impact of AAV-mediated manipulation of PKA-Rap1-MEK pathway in accumbal D2R-MSN on aversive behaviors in passive avoidance tests and real-time place aversion tests. Our findings suggested that accumbal D2R-MSNs regulate aversive behaviors through the A2aR-PKA-Rap1-MEK pathway.

2. Materials and methods

2.1. Animals

All mice were kept at a density of four mice per cage (17 cm wide × 28 cm long × 13 cm high) in a specific pathogen-free animal facility under standard conditions (23 ± 1 °C, 50 ± 5% humidity) with a 12-h light/dark cycle. Food and water were available *ad libitum*. The following male mouse lines at the age of 7 weeks were used for experiments: C57BL/6J jms (Japan SLC, Inc., Shizuoka, Japan), *Drd1-YFP* (RBRC03111, Riken BRC, Tsukuba, Japan), *Drd2-YFP* (RBRC02332, Riken BRC), *DAT-PF-tTA* (027178, Jackson Laboratory, Bar Harbor, ME, USA), *Adora 2a-Cre* (4361654, MMRC, UC Davis, CA, USA) and *Drd1a-Cre* (MMRC, UC Davis, CA, USA). All heterozygous transgenic mice were obtained by crossing heterozygous or homozygous transgenic mice with C57BL/6J jms mice. PCR for genotyping was carried out according to the protocols provided by each company. The primers for genotyping were as followed; *Drd1-YFP*, TCC TGA TGG AAC ACC ATT GTG for primer 1, GCA GAT TAA CTT CAG GGT CAG C for primer 2, CAA ATG TTG CTT GTC TGG TG for primer 3, GTC AGT CGA GTG CAC AGT TT for primer 4; *Drd2-YFP*, CAG TAT CTA TTA TTT CTT TTA GAA CG for primer 1, GCA GAT TAA CTT CAG GGT CAG C for primer 2, CTA GGC CAC AGA ATT GAA AGA TCT for primer 3, GTA GGT GGA AAT TCT AGC ATC ATC C for primer 4; *DAT-PF-tTA*, TGA TGA GGG TGG AGT TGG TC for primer 1, AGA AGA AGG AAA CAG ACT TCC TC for primer 2, GCT TGT TCT TCA CGT GCC AGT for primer 3; *Adora 2a-Cre*, CGT GAG AAA GCC TTT GGG AAG CT for primer 1, CGG CAA ACG GAC AGA AGC ATT for primer 2; *Drd1a-Cre*, GCG GTC TGG CAG TAA AAA CTA TC for primer 1, GTG AAA CAG CAT TGC TGT CAC TT for primer 2, CAC GTG GGC TCC AGC ATT for primer 3, TCA CCA GTC ATT TCT GCC TTT G for primer 4. All animal experiments were approved (reference number: 20094) and performed in the laboratory in accordance with the guidelines for the care and use of laboratory animals established by the animal experiments committee of Nagoya University Graduate School of Medicine. This study was not pre-registered.

2.2. Drugs

KW6002 was purchased from Medchemexpress (HY-10888, Monmouth Junction, NJ, USA). The preparation and dosages of KW6002 were adapted from a previous report (Asaoka et al., 2019) with minor modifications. KW6002 was dissolved in DMSO at 24 mg/ml as a stock solution and stored at −20 °C until use. Stock solution was diluted with 0.001% Tween 80/saline (v/v) to desired working concentrations. Mice were intraperitoneally injected with vehicle (0.001% Tween 80/saline) or KW6002 (0.1 mg/kg and 0.25 mg/kg) 20 min before the training session of the passive avoidance test and returned to the home cage until behavioral experiments.

2.3. Antibodies

The antibody against phosphorylated Rap1gap S563 was previously described (Zhang et al., 2019). The following antibodies were obtained commercially: rabbit anti-Rap1gap (RRID: AB_777621) from Abcam (Cambridge, UK), rabbit anti-phospho-NMDAR1 S897 (RRID: AB_2112139) from Cell Signaling Technology (Danvers, MA, USA), mouse anti-NMDAR1 (RRID: AB_350446) from Novus Biologicals (Colorado, NJ, USA), rat anti-GFP antibody (RRID: AB_10013361) from Nacalai Tesque (Kyoto, Japan), rabbit anti-tyrosine hydroxylase (TH) antibody (RRID:AB_390204) from Millipore (Burlington, MA, USA), mouse anti-RFP (AB_1278880) from MBL Life Science (Aichi, Japan), goat anti-rat Alexa fluor 488 (RRID: AB_2534074), goat anti-rabbit Alexa fluor 568 (RRID: AB_143157) and goat anti-rabbit alexa fluor 680 (RRID: AB_10375714) from Thermo Fisher Scientific (Waltham, MA, USA), and goat anti-mouse IgG (H + L) Dylight 800 conjugate antibody (RRID: AB_10693543) from Cell Signaling Technology.

2.4. Passive avoidance test

Passive avoidance tests were carried out according to previous reports with minor modifications (Yamada et al., 1999; Ögren and Stiedl 2010). The experimental apparatus consisted of one illuminated chamber (25 × 15 × 15 cm high) and one dark chamber with a grid floor. The grid floors consisted of 15 parallel steel rods (0.2 cm in diameter) set 1 cm apart. These two chambers were separated by a guillotine door. On day 0, mice were placed into the illuminated chamber. Fifteen seconds later, the door was opened. When the mouse entered the dark chamber, the door was closed, and the mouse was put back to the home cage. The mice that entered the dark chamber within 1 min were used in subsequent experiments. On day 1, a training session was carried out. Each mouse was placed into the illuminated chamber. Fifteen seconds later, the door was opened. The door was immediately closed after the mice entered the dark chamber, and electric foot shock (0.4 mA, 60 Hz for 2 s or 0.3 mA, 60 Hz for 1 s) was delivered to the grid floor by an isolated stimulator (NS-SG01, Neuroscience, Tokyo, Japan). The step-through latency was recorded. The test session was carried out 24 h after the training session. Each mouse was placed into the illuminated chamber again, and step-through latency was recorded up to a maximum cut-off time of 5 min. All the procedures were conducted within 1 p.m.–5 p.m.

2.5. Immunoblotting

Immediately after decapitation, mice skulls were immersed in liquid nitrogen for 4 s. The brains were removed, and the NAc was punched out onto an ice-cold plate. Each brain tissue sample was immediately frozen

in liquid nitrogen and stored in a freezer at −80 °C until immunoblotting assays. Samples were homogenized in 1% SDS and immediately heated to 99 °C for 10 min. The protein concentration was determined using a Pierce BCA protein assay kit (Thermo Fisher Scientific), and 30 μg protein of each sample was loaded on 10% acrylamide gels. For total protein immunoblotting, 10 μg protein of each sample was loaded on 10% acrylamide gels. After electrophoresis, the proteins were transferred onto a polyvinylidene difluoride membrane (Millipore). Membranes were blocked for 1 h with Blocking-One (Nacalai Tesque) at room temperature and incubated overnight at 4 °C with primary antibodies. Primary antibodies and their dilution were as follows: anti-phospho-Rap1gap S563 (1:1000), anti-Rap1gap (1:1000), anti-phospho-NMDAR1 S897 (1:1000) and anti-NMDAR1 (1:1000). After 3 times wash with tris-buffered saline (TBST; 20 mM Tris, 150 mM NaCl, 0.05% Tween 20, pH 7.6), the membranes were incubated with goat anti-rabbit Alexa fluor 680 or goat anti-mouse IgG (H + L) Dylight 800 conjugate antibody (1: 20,000) at room temperature (RT) for 1 h and washed 3 times with TBST. Signals of antibodies were detected by an infrared imaging system (LI-COR Biosciences, Lincoln, NE, USA). Signal intensities were quantified using Imagestudio software (LI-COR Biosciences). The quantified data were normalized with each total protein.

2.6. Immunohistochemistry

Immunohistochemical analysis was performed according to a previous report (Saifullah et al., 2018). Mice were anesthetized with tribromoethanol (200 mg/kg, i.p.) for rapid and deep anesthesia and further perfused intracardially with isotonic 4% paraformaldehyde (PFA) in PBS, pH 7.4. The brains were post-fixed in 4% PFA overnight at 4 °C. After cryoprotection in 20–30% sucrose in PBS on the following days, samples were frozen using OCT compound (Sakura Finetechnical, Tokyo, Japan). Coronal brain slices (between +0.86 and +1.5 mm from bregma, 20 μm-thick) were fixed with 4% PFA for 5 min and incubated with 0.3% Triton X-100/PBS for 10 min at RT. After three times washes with 0.3% Triton X-100/PBS, the slices were incubated for 1 h at RT in blocking one P (Nacalai Tesque) and stained overnight at 4 °C in the presence of the primary antibody (anti-GFP antibody, 1:500; anti-phospho-Rap1gap S563 antibody, 1:200; anti-TH antibody, 1:500; anti-mCherry, 1:500) diluted in blocking one P. The next day, slices were washed three times with 0.3% Triton X-100/PBS and incubated with the secondary antibody (goat anti-rat Alexa fluor 488, 1:1000; goat anti-rabbit Alexa fluor 568, 1:1000, DAPI 1:2000 in blocking one P) for 1 h at RT. Image acquisition was performed by confocal microscope (LSM780, Carl Zeiss, Jena, Germany) using a 63 × objective with identical pinhole, dwell time, gain, and laser settings. Three sections from each mouse were collected for the analysis. No post-processing was performed on any images, and the number of pRap1gap or YFP-positive cells was quantified using ImageJ software in three sections in each mouse. ROIs (300 μm × 300 μm areas) in the NAc core were acquired at the same focal level. The number of target cells in each ROI was manually counted using the cell counter plugin of the ImageJ software. The results from the ROIs were added to determine the total number of positive cells in the NAc core.

2.7. Plasmid construction and AAV preparation

mCherry was cloned to replace the EGFP of the pAAV-CAGGS-Flex-EGFP-P2A-MCS-WPRE (Nagai et al., 2016a). PKAwt, PKAca, PKAdn (Imai et al., 2006; Orellana and Mcknight 1992), Rap1wt, Rap1ca, and SPA1ca were each cloned into the multiple cloning site (MCS) of the pAAV-CAGGS-Flex-mCherry-P2A-MCS-WPRE. PKAdn and SPA1ca were each cloned into the MCS of the pAAV-CAGGS-Flex-EGFP-P2A-MCS-WPRE. We cloned mCherry and ArchT from pAAV-TetO(3G)-ArCHT-EGFP into pTREtight2 (Addgene plasmid # 19407, RRID: addgene_19407). The preparation of AAV vectors was as previously described (Sooksawate et al., 2013). AAV plasmids, pHelper (Cell Biolabs, Inc., SD, CA), and pAAV-DJ (Cell Biolabs, Inc.) were transfected into AAV293 cells (Cell Biolabs, Inc.). After 72 h incubation, cells were collected, and the viruses were purified by two times CsCl-gradient ultracentrifugation. CsCl was subsequently removed by dialysis. AAV titers were estimated via qPCR. After titration, the concentration of AAV virus solution was diluted to 1.0×10^{12} genome copies/mL. The illustrations of AAV injection site were shown in Fig. S1.

2.8. Surgery

Stereotaxic injections were performed on 7-week-old mice with tribromoethanol (250 mg/kg, i.p.) anesthesia using a stereotaxic instrument (David Kopf, Tujunga, CA, USA). A concentrated AAV virus solution (0.5 μL, 1.0×10^{12} genome copies/mL) was injected into the NAc through a glass capillary at a 10° angle and a rate of 0.1 μL/min (0.5 μL/site, four sites: bregma +1.6, ±1.5, and −4.4; and +1.0, ±1.6, and −4.5.) or VTA/SNc (0.5 μL/site, two sites: bregma −3.1, ±0.5 and −4.5). To manipulate in accumbal D2R-MSN, AAV-FLEX-mutant PKA or SPA1 was injected into the NAc of *Adora2a-Cre* transgenic mice. In accumbal D1R-MSN manipulation, AAV-FLEX-mutant PKA or SPA1 was injected into the NAc of *Drd1a-Cre* transgenic mice. For the manipulation of mesolimbic DAergic neurons, AAV-tetO-ArchT was injected into the VTA/SNc of *DAT-PF-tTA* transgenic mice. Three weeks after virus injection, the mice were subjected to the following experiments. For real-time conditioned place aversion test, an optic fiber guide cannula (diameter is 500 μm, Eicom, Kyoto, Japan) was placed at least 500 μm above the NAc and cemented onto the skull using dental cement (Kuraray, Ibaraki, Japan). After surgery, a dummy cannula (diameter is 350 μm, Eicom, Kyoto, Japan) was inserted into the optic fiber cannula until the behavioral test. Mice were allowed at least 3 weeks to recover and to express the virus before behavioral experiments.

2.9. Real-time conditioned place aversion test

Real-time conditioned place aversion test was done according to previously reported methods (Zhu et al., 2016). The experimental apparatus consisted of two compartments: an illuminated plexiglass chamber and a dark plexiglass chamber (W 16 cm × D 16 cm × H 17 cm). To render the mice being able to distinguish these two chambers, the floor of the white chamber was an uneven plexiglass and the floor of the black chamber was a smooth black plexiglass. All sessions were conducted under conditions of dim illumination (40 lux). After connecting the optical fiber (370 μm, Eicom, Kyoto, Japan), the mice were placed in the experimental apparatus for 15 min to record their baseline place preference without laser stimulation (Zhu et al., 2016). One side of the chamber was randomly assigned as the laser stimulation side. One hour after the baseline recording session, mice were put in the non-light stimulation side, and the time spent in each compartment was recorded. When the mouse entered the light stimulation side of the chamber, yellow light was delivered to the NAc (575 nm, 20 ms pulses, 20 Hz) until the mouse left the stimulation side. Place aversion score was calculated by subtracting the time spent in the stimulation side during the baseline (without light stimulation) from the time spent in the stimulation side during the test (with light stimulation).

2.10. Experimental design and statistical analysis

Time-line diagrams of the experiment were shown in figures. Randomization and blinding were not carried out in brain punch out samples. Behavioral experiments were conducted using experimentally naive animals. No animals were excluded from analyses. The sample sizes were not pre-determined. The sample number of passive avoidance test are referred to Ögren and Stiedl (2010). Slices were obtained from a minimum of 3 different animals. All data are expressed as the mean ± SEM. One-way or two-way analysis of variance (ANOVA) was used,

followed by the Tukey test when the F ratios were significant ($p < 0.05$). Student's-t test was used to determine the significance of comparisons between two groups. Statistical analyses were conducted in Prism 6.0 (Graphpad software, San Diego, CA, USA).

3. Results

3.1. Aversive stimulus activates PKA-Rap1 signaling in the NAc of mice

To examine whether an aversive stimulus activates PKA in the NAc as previously suggested (Nakanishi et al., 2014), we monitored the phosphorylation level of NMDA receptor GluN1 subunit S897, which is a well-known PKA substrate, in C57BL/6J mice after exposure to electric foot shock (0.4 mA, 60 Hz, 2 s) (Fig. 1A). The phosphorylation level of GluN1 S897 significantly increased 15, 30, and 60 min after the electric foot shock compared with non-foot shocked control mice ($p < 0.01$ for 15 and 60 min, $p < 0.05$ for 30 min, Fig. 1B). Next, we analyzed the phosphorylation level of Rap1gap S563 in the NAc after exposure to foot shock. The phosphorylation of Rap1gap S563 was promoted 15 min after the foot shock exposure, and a significant increase in the phosphorylation level was detected 30 min after the exposure compared with control mice ($p < 0.01$, Fig. 1C). These results indicated that the PKA-Rap1 signaling in the NAc was activated by aversive stimulus.

3.2. A2aR mediates Rap1gap phosphorylation evoked by aversive stimulus

It is well-known that A2aR is selectively and highly expressed in D2R-MSNs of the NAc (Stockwell et al., 2017). We speculated that A2aR might be the key receptor that activates the PKA-Rap1 signaling caused by aversive stimulus in the NAc. We injected an A2aR antagonist KW6002 or vehicle (0.001% Tween 80/saline) to C57BL/6J mice 20 min before electric foot shock (0.4 mA, 60 Hz, 2 s) and monitored Rap1gap S563 phosphorylation in the NAc (Fig. 2A). The electric foot shock promoted the phosphorylation levels of Rap1gap S563 in the NAc of vehicle-treated mice ($p < 0.01$, Fig. 2B). The electric foot shock-evoked Rap1gap S563 phosphorylation was inhibited by pretreatment with KW6002 ($p < 0.05$, Fig. 2B). KW6002 itself had no effect on the phosphorylation level of Rap1gap S563 (Fig. 2B).

To determine whether Rap1gap phosphorylation in accumbal D2R-MSNs responds to aversive stimulus, we investigated the anatomical expression profile of phosphorylated Rap1gap-positive cells in the NAc of *Drd2-YFP* transgenic mice, in which D2R-MSNs express a variant of YFP. The number of phosphorylated Rap1gap S563-positive cells in the

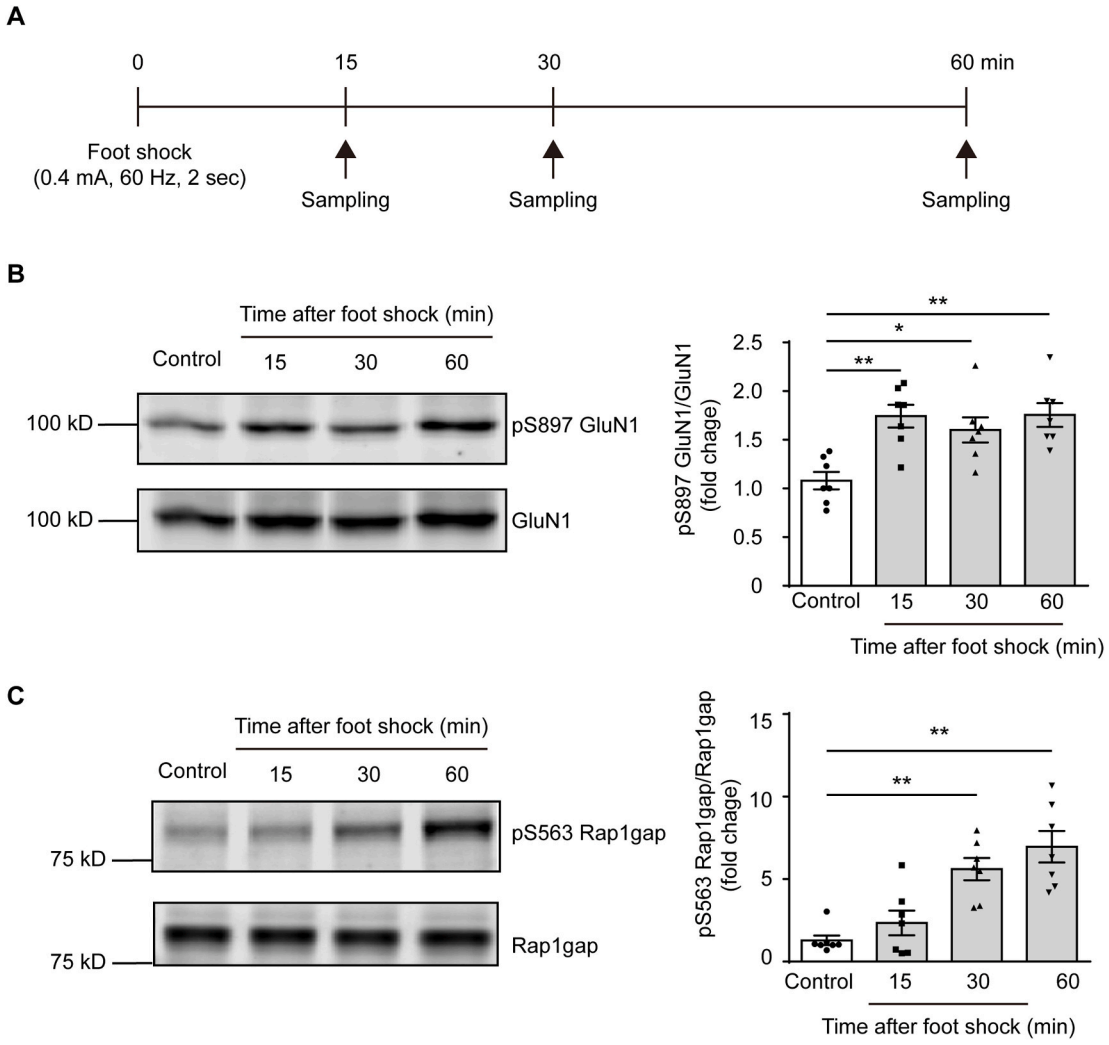

Fig. 1. Aversive stimulus activates PKA-Rap1 signaling in the NAc of mice. (A) Time-line diagram. C57BL/6J mice were exposed to electric foot shock (0.4 mA, 60 Hz, 2 s). The phosphorylation level of Rap1gap S563 and GluN1 subunit S897 in the NAc were measured 15, 30, and 60 min after the foot shock. (B, C) Electric foot shock increased the phosphorylation level of NMDA receptor GluN1 subunit (B) and Rap1gap (C). Left panels show representative immunoblots. Quantification of the immunoblotting assay is shown in the right panels. Data are represented as the mean ± SEM (n = 7 for each group). One-way ANOVA; $F(3, 24) = 14.23$, $p < 0.01$ for Fig. 1B; $F(3, 24) = 7.57$, $p < 0.01$ for Fig. 1C. *$p < 0.05$ and **$p < 0.01$.

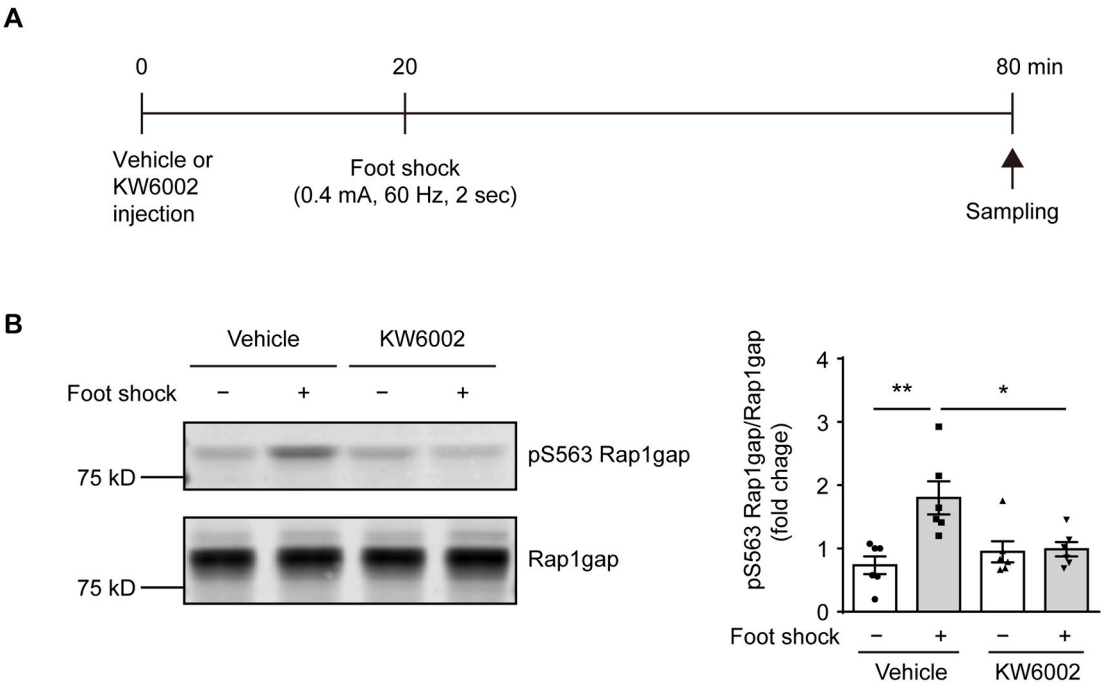

(caption on next page)

Fig. 2. A2aR mediates Rap1gap phosphorylation evoked by aversive stimulus. (A) Time-line diagram. We intraperitoneally injected an A2aR antagonist KW6002 (0.25 mg/kg) or vehicle (0.001% Tween 80/saline) to C57BL/6J or *Drd2-mVenus* transgenic mice 20 min before electric foot shock (0.4 mA, 60 Hz, 2 s) and monitored Rap1gap S563 phosphorylation in the NAc. (B) A2aR antagonist KW6002 inhibited phosphorylation of Rap1gap S563 after electric foot shock. Left panels show representative immunoblots. Quantification of the immunoblotting assay is shown in the right panels. Data are represented as the mean ± SEM (n = 6 for each group). Two-way ANOVA; foot shock, $F(1, 20) = 9.449$, $p = 0.006$; A2aR antagonist, $F(1, 20) = 2.776$, $p = 0.111$; interaction, $F(1, 20) = 8.178$, $p = 0.010$. (C–E) Rap1gap phosphorylation was detected in accumbal D2R-MSNs after electric foot shock. Rap1gap phosphorylation was inhibited by the pretreatment with A2aR antagonist. The diagrammatic representation shows the brain area examined for immunohistochemical analysis (left panel). The red square indicates the region of interest. Immunofluorescence staining image using the anti-phosphorylated Rap1gap S563 (upper panel) or overlay of anti-phosphorylated Rap1gap S563, anti-GFP antibody, and DAPI (bottom panels) is shown. Magenta, phosphorylated Rap1gap S563; green, D2R-MSN; blue DAPI. Scale bar indicates 20 μm. Quantification of phosphorylated Rap1gap S563-positive cells is shown (D). Two-way ANOVA; foot shock, $F(1, 8) = 32.75$, $p < 0.001$; A2aR antagonist, $F(1, 8) = 33.58$, $p < 0.001$; interaction, $F(1, 8) = 27.17$, $p = 0.001$. (E) Percentage of phosphorylated Rap1gap S563 and YFP double-positive cells in all YFP-positive cells in each mouse. Data are represented as the mean ± SEM (n = 3 for each group). Two-way ANOVA; foot shock, $F(1, 8) = 44.6$, $p < 0.001$; A2aR antagonist, $F(1, 8) = 38.6$, $p < 0.001$; interaction, $F(1, 8) = 37.01$, $p < 0.001$. *$p < 0.05$ and **$p < 0.01$.

NAc significantly increased in vehicle-treated *Drd2-YFP* transgenic mice 60 min after exposure to electric foot shock (0.4 mA, 60 Hz, 2 s) compared with that in vehicle-treated control mice without electric foot shock ($p < 0.05$, Fig. 2C and D). The electric foot shock-evoked phosphorylation of Rap1gap S563 was dominant in D2R-MSNs of vehicle-treated *Drd2-YFP* transgenic mice ($p < 0.05$, Fig. 2C and E). Pretreatment with KW6002 decreased the number of phosphorylated Rap1gap S563-positive cells evoked by the electric foot shock ($p < 0.05$, Fig. 2C–E). A similar experiment was performed in *Drd1a-YFP* transgenic mice. A significant increase in the number of phosphorylated Rap1gap S563-positive cells was observed after electric foot shock exposure (Fig. S2). However, phosphorylated Rap1gap S563 immunoreactivity co-localized to non-D1R–YFP cells in the NAc of *Drd1a-YFP* transgenic mice. These results suggested that aversive stimulus activates PKA-Rap1 signaling mainly through A2aR in accumbal D2R-MSNs but not D1R-MSNs.

3.3. Inhibition of PKA-Rap1 signaling in accumbal D2R-MSNs impairs aversive memory in passive avoidance test

It is well-known that aversive experiences easily form negatively charged memory (Hamann et al., 1999; Harris and Pashler 2005; Hoscheidt et al., 2014; Meyer and Louilot 2014). Aversive memory may be affected by the activation or inactivation of A2aR-PKA-Rap1 signaling in accumbal D2R-MSNs following aversive stimulus. To further understand the causal relationship between signaling pathway and aversive behaviors, we performed passive avoidance tests, which are fear-motivated tests classically used to assess memory on laboratory animals (Ader et al., 1972; Drago et al., 1999; Ögren and Stiedl 2010). Mice were administered KW6002 20 min before training sessions with electric foot shock (0.4 mA, 60 Hz, 2 s) of the passive avoidance test, and step-through latency was recorded in the test session 24 h after training (Fig. 3A). Vehicle-treated mice showed a marked increase in the step-through latency in the test session (Fig. 3B). KW6002 decreased the step-through latency in a dose-dependent manner, indicating an impairment of aversive memory ($p < 0.05$, Fig. 3B).

To further investigate the role of PKA in D2R-MSNs, we established a system in which dominant negative mutant PKA (PKAdn) was expressed in the NAc under the control of the A2aR promoter gene (*Adora2a*) using adeno-associated virus (AAV)-mediated flip-excision (FLEX) conditional transgenic techniques (Fig. 3C and D). The PKAdn is a cAMP-binding domain that leads to the inhibition of PKA activity [G324D] (Clegg et al., 1987; Correll et al., 1989). Three weeks after the AAV injection, *Adora2a-Cre* transgenic mice were subjected to the passive avoidance test. Compared with an mCherry-expressed control group, *Adora2a-Cre* mice expressing PKAdn showed significantly decreased step-through latency ($p < 0.01$, Fig. 3D). When DA D1R promoter gene (*Drd1a*) transgenic mice were injected with AAV-PKAdn into the NAc, no significant differences were observed between PKAdn and the mCherry-expressed control in the *Drd1a-Cre* mice (Fig. S3). We monitored the effect of constitutive active mutant SPA1 (SPA1ca), which is a RapGAP and can inactivate Rap1 (Fig. 3E). SPA1ca was used in the present study to inhibit the Rap1 activity in D2R-MSNs instead of dominant negative mutant Rap1 (Rap1dn) because Rap1dn has been reported to fail to bind to Rap1 GEFs (Reedquist et al., 2000; Berghe et al., 1997). SPA1ca-transfected *Adora2a-Cre* transgenic mice showed memory impairment in the passive avoidance test ($p < 0.01$, Fig. 3E). Both PKAdn and SPA1ca had no effect on pain threshold levels in the *Adora2a-Cre* transgenic mice (Figs. S4A and B). These results indicated that the inhibition of A2aR-PKA-Rap1 signaling pathway in D2R-MSNs impairs aversive memory.

3.4. Activation of PKA-Rap1 signaling in accumbal D2R-MSN enhances aversive memory

We investigated whether activation of PKA-Rap1 signaling in accumbal D2R-MSN could enhance aversive memory. *Adora2a-Cre* transgenic mice were injected with AAV encoding wild-type PKA (PKAwt), constitutively active mutant PKA (PKAca), wild-type Rap1 (Rap1wt), or constitutively active mutant Rap1 (Rap1ca) into the NAc. PKAca is a PKA catalytic subunit that is not regulated by cAMP [H87Q and W196R] (Orellana and Mcknight 1992). Rap1ca is a fast-cycling variant of Rap1a [F28L] (Reinstein et al., 1991). Three weeks later, training sessions in the passive avoidance test with low level electric foot shocks (0.3 mA, 60 Hz, 1 s) were carried out, and step-through latency was recorded in test sessions 24 h after the training (Fig. 4A and B). As expected, the step-through latency of PKAca or Rap1ca-expressed *Adora2a-Cre* transgenic mice significantly increased compared with mCherry-expressed control mice ($p < 0.01$ and $p < 0.05$, respectively, Fig. 4C and D). The PKAwt and Rap1wt-expressed *Adora2a-Cre* transgenic mice also showed an increase in step-through latency, but not significant, compared with mCherry-expressed control mice (Fig. 4C and D). Both PKAca and Rap1ca had no effect on pain threshold levels in the *Adora2a-Cre* transgenic mice (Fig. S4C). These results indicated that activation of PKA-Rap1 signaling in accumbal D2R-MSN facilitates aversive memory.

3.5. MAPK signaling in accumbal D2R-MSN mediates aversive memory

MAPK1/3 (also ERK1/2) is known to be activated by Rap1 by activating B-raf-MEK1/2 signaling (Nagai et al., 2016a; Waltereit and Weller 2003). Therefore, to further examine the role of MAPK signaling in aversive memory, we investigated the effects of dominant negative mutant MEK1 (MEK1dn) or constitutively active mutant MEK1 (MEK1ca) expression in accumbal D2R-MSN on the performance in passive avoidance tests (Fig. 5A and B). MEK1dn-transfected *Adora2a-Cre* transgenic mice showed reduced step-through latency in the test session of the passive avoidance test ($p < 0.01$, Fig. 5C). Conversely, the step-through latency of MEK1ca-transfected *Adora2a-Cre* transgenic mice increased compared with that of control mice ($p < 0.01$, Fig. 5D), suggesting that MAPK1/3 in accumbal D2R-MSN may be one downstream PKA-Rap1 molecule that mediates aversive memory.

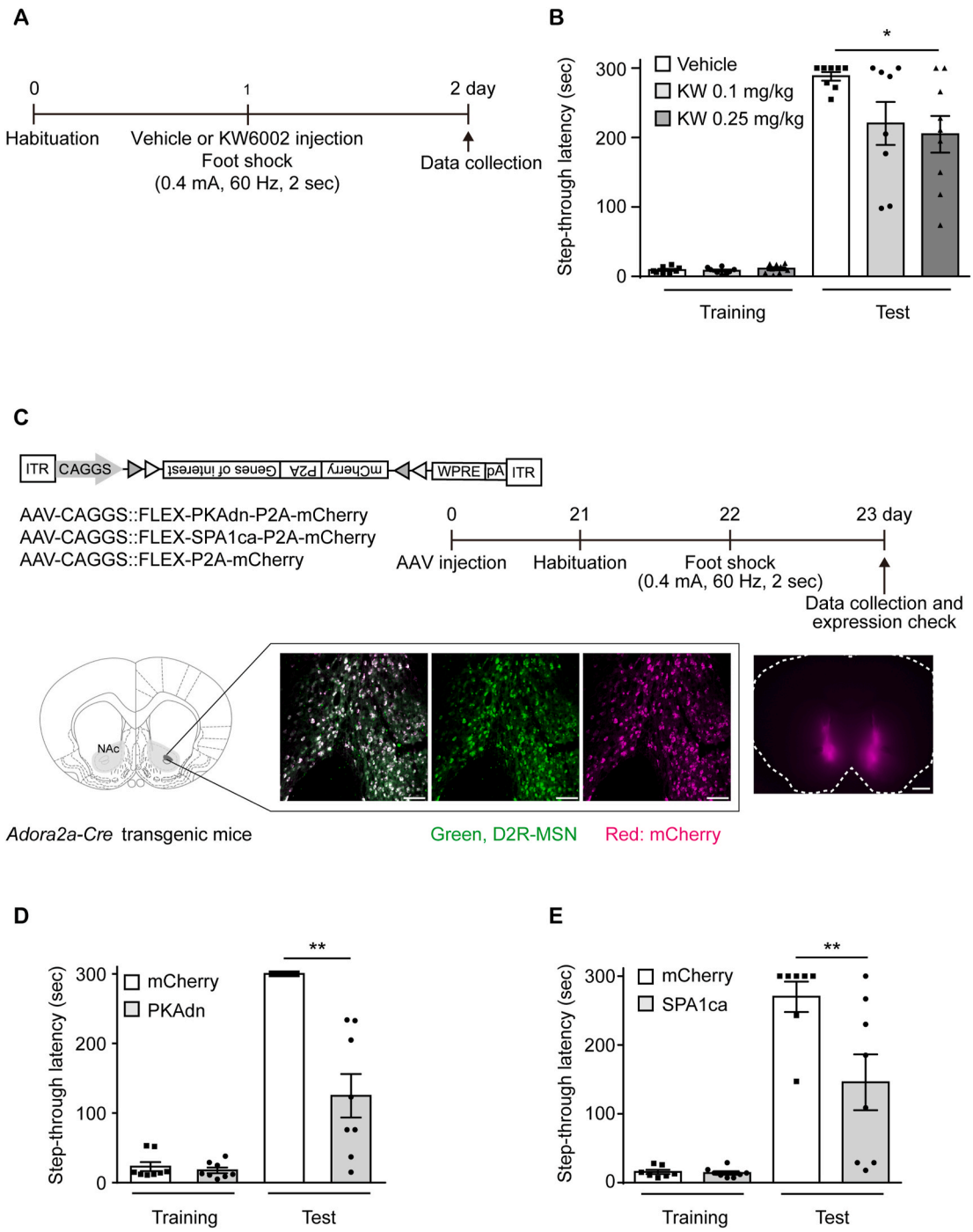

Fig. 3. Inhibition of A2aR-PKA-Rap1 signaling in accumbal D2R-MSN impairs aversive memory in passive avoidance tests. (A, B) A2aR antagonist decreased step-through latency in passive avoidance tests. (A) Time-line diagram. (B) Step-through latency in passive avoidance tests. Data are represented as the mean ± SEM (n = 8 for vehicle-treated control and 0.1 mg/kg KW6002-treated group, n = 9 for 0.25 mg/kg KW6002-treated group). Two-way ANOVA; training, $F(1, 44) = 266.9$, $p < 0.001$; A2aR antagonist, $F(2, 44) = 3.283$, $p = 0.047$; interaction, $F(2, 44) = 3.435$, $p = 0.041$. (C–E) AAV-mediated expression of PKAdn or SPA1ca in D2R-MSNs decreased step-through latency. (C) Time-line diagram. *Adora2a-Cre* mice were injected with AAV encoding PKAdn or SPA1ca mutant. Passive avoidance tests were carried out 3 weeks after the AAV injection. During the training session, mice were given electric foot shock (0.4 mA, 60 Hz, 2 s) following the measurement of step-through latency. The test session was carried out 24 h after the training session. Schematic of AAV-mediated PKAdn and SPA1ca expression in accumbal D2R-MSNs. The diagram shows the AAV constructs (upper left panel) and stereotaxic injection of AAVs into the NAc of *Adora2a-Cre* transgenic mice (bottom left panel). Representative coronal brain slices showing the expression of mCherry 3 weeks after AAV injection into the NAc (bottom middle and right panel). Representative coronal image of mCherry expression in D2R-MSNs (green color) of the NAc (bottom middle panel). The scale bars indicate 100 μm (bottom middle panel), 1 mm (bottom right panel). (D, E) Step-through latency of PKAdn (D) or SPA1ca (E)-injected *Adora2a-Cre* mice. Data are represented as the mean ± SEM (n = 8 for control/*Adora2a-Cre*, PKAdn/*Adora2a-Cre* for Fig. 3D; n = 7 for control/*Adora2a-Cre* and n = 8 for SPA1ca/*Adora2a-Cre* for Fig. 3E). Two-way ANOVA; training, $F(1, 28) = 142.8$, $p < 0.001$; PKAdn, $F(1, 28) = 31.54$, $p < 0.001$; interaction $F(1, 28) = 27.9$, $p < 0.001$ for Fig. 3D; training, $F(1, 26) = 63.9$, $p < 0.001$; SPA1ca, $F(1, 26) = 6.777$, $p = 0.015$; interaction, $F(1, 26) = 6.439$, $p = 0.018$ for Fig. 3E. **$p < 0.01$.

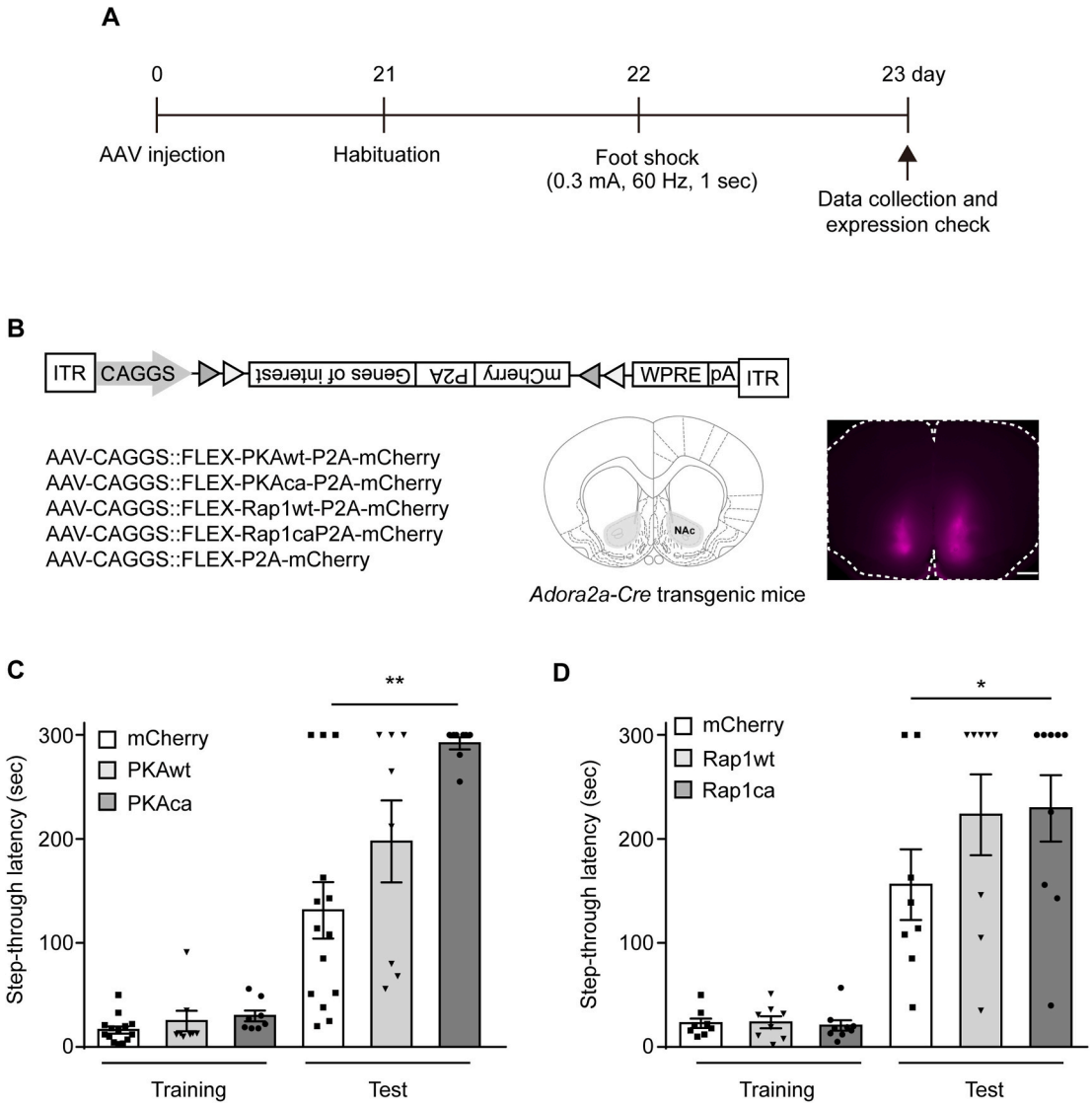

Fig. 4. Activation of PKA-Rap1 signaling in accumbal D2R-MSN enhances aversive memory. (A) Time-line diagram. *Adora2a-Cre* mice were injected with AAV encoding PKAwt, PKAca, Rap1wt, or Rap1ca mutant. Passive avoidance tests were carried out 3 weeks after the AAV injection. During the training session, mice were given electric foot shock (0.3 mA, 60 Hz, 1 s) following the measurement of step-through latency. The test session was carried out 24 h after the training session. (B) Schematic of AAV-mediated PKA and Rap1 expression in accumbal D2R-MSNs. The diagram shows the AAV constructs (upper and left panel) and stereotaxic injection of AAVs into the NAc of *Adora2a-Cre* transgenic mice (right panel). Representative coronal brain slices showing the expression of mCherry 3 weeks after AAV injection into the NAc (right panel). The scale bars indicate 1 mm. (C, D) AAV-mediated expression of PKAwt and PKAca (C) or Rap1wt and Rap1ca (D) in D2R-MSNs potentiated step-through latency. Data are represented as the mean ± SEM (n = 14 for control/*Adora2a-Cre*, n = 8 for PKAwt/*Adora2a-Cre* and PKAca/*Adora2a-Cre* for Fig. 4C; n = 14 for control/*Adora2a-Cre*, n = 8 for Rap1wt/*Adora2a-Cre* and n = 9 for Rap1ca/*Adora2a-Cre* for Fig. 4D). Two-way ANOVA; training, $F(1, 54) = 109.2$, $p < 0.001$; PKA mutant, $F(2, 54) = 9.012$, $p < 0.001$; interaction, $F(2, 54) = 6.393$, $p = 0.003$ for Fig. 4C; training, $F(2, 56) = 83.360$, $p < 0.001$; Rap1 mutant, $F(2, 56) = 3.668$, $p = 0.032$; interaction, $F(2, 56) = 2.885$ $p = 0.064$ for Fig. 4D.*$p < 0.05$ and **$p < 0.01$.

3.6. Inhibition of PKA-Rap1 signaling in accumbal D2R-MSN attenuates the aversive response caused by optogenetic inactivation of mesolimbic DAergic neurons

DAergic activity in the ventral tegmental area (VTA) has been reported to decrease after aversive stimulus or absence of a predicted reward (Cohen et al., 2012; Matsumoto and Hikosaka 2009; Mirenowicz and Schultz 1996; Ungless et al., 2004). Optogenetic activation of the striatal D2R-MSNs induces avoidance behavior (Kravitz et al., 2012). We previously showed that adenosine positively regulates PKA in D2R-MSNs through A2aR, whereas this effect is blocked by basal DA in the NAc (Zhang et al., 2019). These findings raised the possibility that activating A2aR-PKA-Rap1-MAPK signaling in accumbal D2R-MSNs following hypofunction of mesolimbic DAergic neurons enhanced aversive response to stimulus thereby promoting aversive memory. To demonstrate our hypothesis, we applied an optogenetic technique to inhibit mesolimbic DAergic neurons. ArchT-mCherry was expressed in the VTA/SNc under the control of the DA transporter (DAT) promoter gene (*Slc6a3*) using AAV-mediated conditional transgenic techniques (Fig. 6A). Immunohistochemistry revealed exclusive expression of ArchT-mCherry with a DAergic neuronal marker TH (Fig. 6B). To manipulate D2R-MSNs, we injected AAV-PKAdn or SPA1ca, and AAV-tetO-ArchT-mCherry into the NAc and VTA/SNc of *Adora2a-Cre::DAT-PF-tTA* double transgenic mice, respectively. Real-time place aversion test was carried out 3 weeks after the AAV injection (Fig. 6C). Optogenetic inhibition of the mesolimbic DAergic pathway reduced the time spent in a chamber with yellow light stimulation ($p < 0.05$, Fig. 6C). No changes in locomotor activity was observed among all

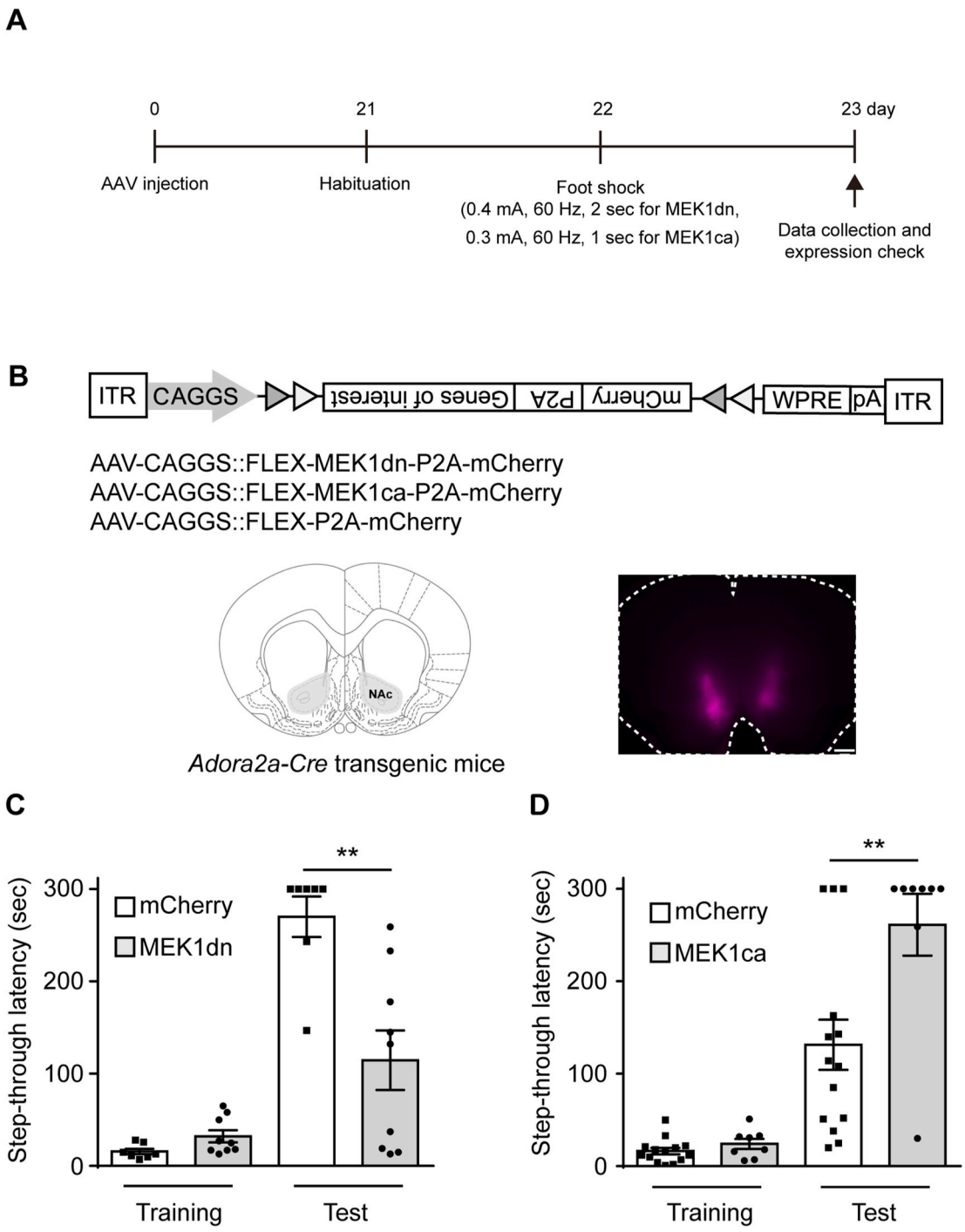

Fig. 5. MAPK signaling in accumbal D2R-MSN mediates aversive memory. (A) Time-line diagram. *Adora2a-Cre* mice were injected with AAV encoding MEK1dn or MEK1ca mutant. Passive avoidance tests were carried out 3 weeks after the AAV injection. During the training session, mice were given electric foot shock (0.4 mA, 60 Hz, 2 s for MEK1dn, 0.3 mA, 60 Hz, 1 s for MEK1ca) following measurement of step-through latency. The test session was carried out 24 h after training session. (B) Schematic of AAV-mediated MEK1 expression in accumbal D2R-MSNs. The diagram shows the AAV constructs (upper panel) and stereotaxic injection of AAVs into the NAc of *Adora2a-Cre* transgenic mice (bottom left panel). Representative coronal brain slices showing the expression of mCherry 3 weeks after AAV injection into the NAc (bottom right panel). The scale bars indicate 1 mm. (C) AAV-mediated expression of MEK1dn reduced step-through latency. (D) AAV-mediated expression of MEK1ca in D2R-MSNs extended step-through latency. Data are represented as the mean ± SEM (n = 7 for control/*Adora2a-Cre*, n = 8 for MEK1dn/*Adora2a-Cre* for Fig. 5C; n = 14 for control/*Adora2a-Cre*, n = 8 for MEK1ca/*Adora2a-Cre* for Fig. 5D). Two-way ANOVA; training, $F(1, 28) = 62.81$, $p < 0.001$; MEK1dn, $F(1, 28) = 10.7$, $p = 0.003$; interaction, $F(1, 28) = 16.39$, $p < 0.001$ for Fig. 5C; training, $F(1, 40) = 62.72$, $p < 0.001$; MEK1ca, $F(1, 40) = 9.606$, $p = 0.004$; interaction, $F(1, 40) = 7.512$, $p = 0.009$ for Fig. 5D. **$p < 0.01$.

groups in real-time place aversion test (Fig. S5). These results indicate that inhibiting mesolimbic DAergic neuron causes aversive behavior. This aversive response was suppressed by PKAdn and SPA1ca expression in accumbal D2R-MSNs ($p < 0.01$ and $p < 0.05$, respectively, Fig. 6C). These data clearly indicated that PKA-Rap1 signaling in accumbal D2R-MSNs controls aversive response.

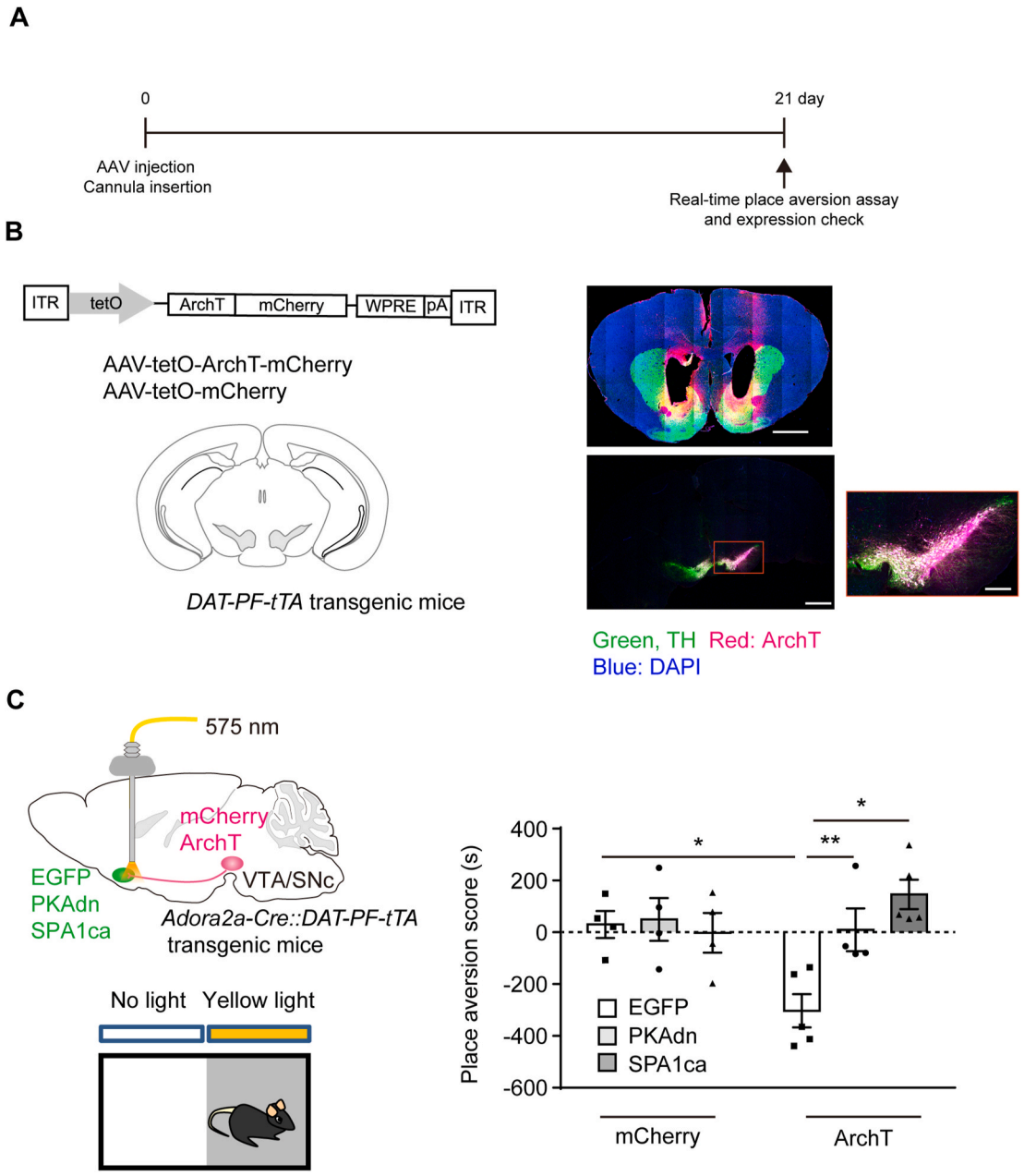

Fig. 6. Inhibition of PKA-Rap1 signaling in accumbal D2R-MSN attenuates the aversive response caused by the inactivation of DAergic neurons in real-time place aversion test. (A) Time-line diagram (B) Schematic of AAV-mediated inactivation of DAergic neurons. The diagram shows the AAV constructs (upper left panel) and stereotaxic injection of AAVs into the VTA/SNc of *DAT-PF-tTA* transgenic mice (bottom left panel). Representative coronal brain slices showing the expression of mCherry (red), TH (green), and DAPI staining (blue) in the NAc (upper right panel) and VTA/SNc (bottom middle panel) 3 weeks after AAV injection of tetO-ArchT-mCherry into the VTA/SNc. The scale bar indicates 1 mm. Large magnification of VTA/SNc was shown in bottom right panel. The scale bar indicates 200 μm. (C) Expression of PKAdn and SPA1ca in accumbal D2R-MSNs attenuates the aversive response induced by light-stimulus in real-time place aversion test. *Adora2a-Cre::DAT-PF-tTA* double transgenic mice were injected AAV encoding PKAdn or SPA1ca into the NAc, and tetO-ArchT into the VTA/SNc (upper left panel). Mice were subjected to real-time place aversion test 3 weeks after the AAV injection (bottom left panel). Place aversion scores of AAV-injected mice were shown in the right panel. Data are represented as the mean ± SEM (n = 4 for mCherry-EGFP/*Adora2a-Cre::DAT-PF-tTA*, mCherry-PKAdn/*Adora2a-Cre::DAT-PF-tTA*, mCherry-SPA1ca/*Adora2a-Cre::DAT-PF-tTA*, ArchT-SPA1ca/*Adora2a-Cre::DAT-PF-tTA* and n = 5 for ArchT-EGFP/*Adora2a-Cre::DAT-PF-tTA*, ArchT-PKAdn/*Adora2a-Cre::DAT-PF-tTA*). Two-way ANOVA; ArchT, $F(1, 20) = 1.738$, $p = 0.202$; mutants, $F(2, 20) = 5.186$, $p = 0.015$; interaction, $F(2, 20) = 6.325$, $p = 0.007$. *$p < 0.05$ and **$p < 0.01$.

4. Discussion

The basal ganglia circuit, which includes mesolimbic DAergic neurons, has long been implicated in positive and negative reinforcements, such as reward-related behaviors, addiction, aversive processing, and depression. However, the encoding of aversive processing in this circuit remains largely unclear. In this study, we proposed a new perspective on the balance between activation of A2aR and inactivation of D2R in accumbal D2R-MSN using a combination of neurochemical, histochemical, AAV expression system, optogenetics, and behavioral techniques. In basal condition, adenosine tonically stimulates PKA-Rap1 through A2aR, but the activation of PKA-Rap1 is inhibited by D2R activation under basal DA concentration. The decrease of dopamine release and the subsequent inactivation of D2R in response to aversive stimuli activates PKA-Rap1 signaling due to disinhibition. Thus, the NAc may mediate aversive behavior through the A2aR-PKA-Rap1 signaling

pathway following the reduction of DA release from mesolimbic DAergic neurons in the NAc after aversive stimuli (Fig. 7). Furthermore, we found evidence that MAPK signaling pathway in accumbal D2R-MSN plays a role in aversive behaviors.

The phosphorylation levels of NMDA receptor GluN1 subunit at S897 and Rap1gap S563 have been used to monitor PKA activity because they are well-known PKA substrates (Maldve et al., 2002; Zhang et al., 2019). Phosphorylation of NMDA receptor GluN1 subunit S897 by PKA is required for the surface expression of GluN1 followed by alteration of the size and threshold of synaptic plasticity (Scott et al., 2001). The phosphorylation of Rap1gap S563 inactivates its GAP activity (McAvoy et al., 2009). Therefore, Rap1gap is a strongly recommended candidate for observing the activity of both PKA and Rap1 activity. *In vivo* FRET imaging reveals that PKA activation is observed in accumbal D2R-MSNs when mice are exposed to electric foot shock (Yamaguchi et al., 2015). Zhang et al. (2019) found that the phosphorylation of NMDA receptor GluN1 subunit S897 and Rap1gap S563 are promoted by A2aR agonists in striatal slices. In the present study, phosphorylation levels of NMDA receptor GluN1 subunit S897 and Rap1gap S563 increased in the NAc of mice exposed to electric foot shock (Fig. 1), indicating that the aversive stimulus activates PKA-GluN1 and the PKA-Rap1 signaling pathway in the NAc.

We previously reported that A2aR-stimulated Rap1gap S563 phosphorylation is inhibited by D2R agonists in striatal slices (Zhang et al., 2019). However, the role of A2aR signaling in aversive behavior remains unclear. Here, we demonstrated that electric foot shock-evoked phosphorylation of Rap1gap S563 was evident in D2R-MSNs of the NAc and that this phosphorylation was inhibited by A2aR antagonist KW6002. This suggests that A2aR in accumbal D2R-MSN is the upstream receptor involved in aversive responses. In fact, A2aR antagonist attenuated aversive memory and reduced PKA-Rap1 signaling caused by electric footshock in accumbal D2R-MSNs. These findings indicate that A2aR is a trigger that promotes PKA-Rap1 signaling after aversive stimuli.

To investigate how PKA-Rap1 signaling contributes to aversive behavior, we used AAV-mediated cell-type specific PKA and Rap1 manipulation in accumbal D2R-MSNs. Inhibition of PKA-Rap1 signaling suppressed the step-through latency in passive avoidance tests, whereas the activation of PKA-Rap1 signaling potentiated the latency. PKA-mutant-injected *Adora2a* mice showed an equal pain threshold level to control mice. These results indicated that PKA-Rap1 signaling controls aversive memory and that this is not due to a sensitivity to nociceptive pain.

Previous studies have reported that Rap1 is associated with synaptic plasticity and mental disorders (Pan et al., 2008; Stornetta and Zhu 2011). MAPK1/3 can be activated by PKA-Rap1 signaling cascade (Nagai et al., 2016a; Waltereit and Weller 2003). We also tested the role of MAPK in aversive memory through the AAV-mediated expression of MEK1 mutants. Consistent with previous reports (Shalin et al., 2004),

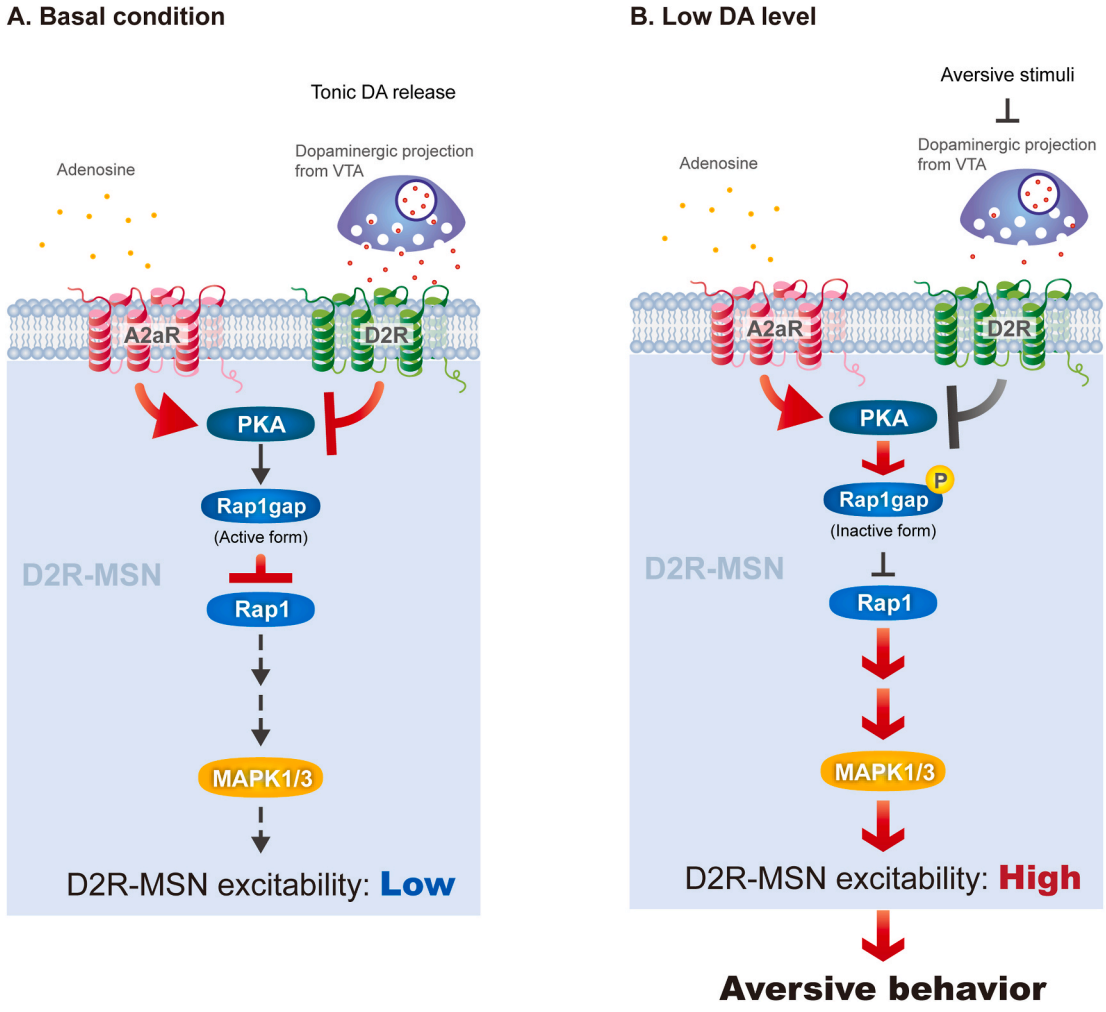

Fig. 7. Working model of PKA-Rap1 signaling in accumbal D2R-MSN mediating aversive behaviors. (A) Basal condition. Adenosine tonically stimulates PKA-Rap1 through A2aR. The activation of PKA-Rap1 is inhibited by D2R activation under basal DA concentration. Thus, D2R-MSN activity is suppressed (B) Low DA level. A low DA state (e.g., aversive experience). activates D2R-MSN due to the inability of D2R to suppress the PKA-Rap1-MAPK pathway downstream A2aR. The activation of accumbal D2R-MSNs regulates aversive response and memory formation.

MEK1dn attenuated aversive memory, whereas MEK1ca potentiated aversive memory. The A2aR-PKA-Rap1 signaling pathway may promote the processing of aversive memory through MAPK. In accumbal D1R-MSNs, Rap1-MAPK pathway controls the neuronal excitability (Nagai et al., 2016b). MAPK also enhances reward-related learning and memory through Npas4 phosphorylation to increase transcriptional activity (Funahashi et al., 2019). Further studies are underway to investigate the role of MAPK and its downstream targets in accumbal D2R-MSNs.

Inhibition of A2aR, PKA, Rap1, and MEK1 partially suppressed step-through latency in the passive avoidance test (Figs. 3 and 5). DA released from VTA and paraventricular thalamus to NAc contributes to the saliency (Hu 2016; Zhu et al., 2016). It has been reported that DA release from VTA is inhibited by the neurons in the rostromedial tegmental nucleus when rats were given aversive stimuli (Jhou et al., 2009; Sánchez-Catalán et al., 2017). In addition to DAergic input, the NAc also receives several glutamatergic inputs from the ventral hippocampus, basolateral amygdala, prefrontal cortex, and thalamus (Scofield et al., 2016). Serotonin, oxytocin, orexin as well as other neurotransmitters have been shown to regulate the activity of the NAc (Klawonn and Malenka 2018). It has been demonstrated that melanocortin signaling through melanocortin 4 receptors in the anterior part of NAc is critical for assigning negative motivational valence to harmful stimuli (Klawonn et al., 2018). Recent studies illustrate that the lateral and medial part of NAc forms different circuit in controlling reward and aversive response (Yang et al., 2018; de Jong et al., 2019). Thus, PKA-Rap1 pathway in the accumbal D2R-MSNs is one of the key elements which control aversive behavior among various factors involved in aversive behaviors.

D2R-MSN has been reported to be involved in rapid aversive reactions and memory formation (Danjo et al., 2014). PKA inhibition in accumbal D2R-MSN has been shown to decrease aversive memory formation and extinction (Yamaguchi et al., 2015). However, the aversive reaction appears when accumbal D2R-MSN are excited after the suppression of DAergic terminals in NAc (de Jong et al., 2019). Therefore, to further specify the role of A2aR-PKA-Rap1-MAPK signaling in accumbal D2R-MSNs in aversive response, we used optogenetic approaches to inhibit the DAergic activity in the NAc. According to the results of real-time place aversion, the inhibition of PKA-Rap1 signaling in accumbal D2R-MSNs can attenuate aversive response induced by photostimulation. These results suggested that A2aR-PKA-Rap1-MAPK signaling mainly plays a role in aversive response; thus, memory formation is impaired.

Based on the pharmacological and microdialysis analysis in rats, basal adenosine concentrations are estimated to be in the range of 25–250 nM and is capable of tonically activating A2aR (Dunwiddie and Masino 2001). It has been reported that handling as an aversive stimulus did not significantly change extracellular adenosine levels in the NAc of rats although there was no report that A2aR is upregulated in response to aversive stimuli (Nagel and Hauber, 2002). If aversive stimulus alters neither release of adenosine nor expression of A2aR, it is reasonable that inhibition of D2R activates the signaling downstream A2aR.

The deficiencies of aversive behaviors are associated with various neuropsychological disorders, such as anxiety disorders and post-traumatic stress disorder (PTSD) (Borsook et al., 2007; Elman et al., 2018). Our study provides a novel application of an A2aR antagonist that has been approved for the adjunctive treatment of patients with Parkinson's disease (Franco and Navarro 2018) in controlling aversive behaviors. The present study would provide clues to therapeutic strategies for treating neuropsychological disorders.

5. Conclusion

We have recently proposed that the balance between DA and adenosine signals regulates the PKA-Rap1 pathway in D1R-MSNs and D2R-MSNs (Zhang et al., 2019). Basal DA concentration cannot activate D1R but activates D2R to suppress D2R-MSN activity. A high DA state (e.g., reward acquirement and abused drugs intake) activates D1R-MSN and inactivates D2R-MSN, whereas a low DA state (e.g., aversive experience) activates D2R-MSN due to the inability of D2R to suppress the A2aR-PKA-Rap1-MAPK pathway. The activation of accumbal D2R-MSNs regulates aversive response and memory formation. Our findings provide a novel negative reinforcement regulating mechanism managed by the activation of PKA-Rap1 in D2R-MSNs.

Declaration of interests

The authors declare that they have no known competing financial interests or personal relationships that could have appeared to influence the work reported in this paper.

The authors declare the following financial interests/personal relationships which may be considered as potential competing interests:

Author contribution

You-Hsin Lin, Taku Nagai, and Kozo Kaibuchi designed the experiments. You-Hsin Lin, Yukie Yamahashi, Xinjian Zhang, and Md. Omar Faruk collected and analyzed the data. Keisuke Kuroda and Kiyofumi Yamada contributed to the mouse lines. Akihiro Yamanaka contributed to the opotogenetic tequniques. You-Hsin Lin, Taku Nagai, and Kozo Kaibuchi wrote the paper.

CRediT authorship contribution statement

You-Hsin Lin: Conceptualization, Funding acquisition, Formal analysis, Data curation, Writing - original draft. **Yukie Yamahashi:** Funding acquisition, Formal analysis, Data curation. **Keisuke Kuroda:** Formal analysis, Data curation. **Md Omar Faruk:** Funding acquisition. **Xinjian Zhang:** Funding acquisition. **Akihiro Yamanaka:** Formal analysis, Data curation, Approval of the version of the manuscript to be published. **Taku Nagai:** Conceptualization. **Kozo Kaibuchi:** Conceptualization, revising the manuscript critically for important intellectual content.

Declaration of competing interest

The authors declare no conflict of interest.

Acknowledgments

We thank the staff of the Division of Experimental Animals, Nagoya University Graduate School of Medicine, for their technical support and the Division for Medical Research Engineering, Nagoya University Graduate School of Medicine, for the use of their confocal microscopy system and image analysis software. We are grateful to Dr. K. Kobayashi for providing *Drd1a-YFP* and *Drd2-YFP* transgenic mice. This study was supported by AMED under grant nos. JP20dm0207075, JP20dm0307025, and JP20mk0101156; Japan Society for the Promotion of Science (JSPS) KAKENHI grant nos. 17H01380, 17J10615, 19K16370, 20K07965, 20H03428, and 20K07082; MEXT KAKENHI grant no. JP19H05209; Hori Sciences & Arts Foundation (FV2019); Toyoaki Scholarship Foundation and the Takeda Science Foundation.

Appendix A. Supplementary data

Supplementary data to this article can be found online at https://doi.org/10.1016/j.neuint.2020.104935.

References

Ader, R., Weijnen, J.A.W.M., Moleman, P., 1972. Retention of a passive avoidance response as a function of the intensity and duration of electric shock. Psychonomic Sci. 26, 125–128. https://doi.org/10.3758/BF03335453.

Asaoka, N., Nishitani, N., Kinoshita, H., Nagai, Y., Hatakama, H., Nagayasu, K., Shirakawa, H., Nakagawa, T., Kaneko, S., 2019. An adenosine A_{2A} receptor antagonist improves multiple symptoms of repeated quinpirole-induced psychosis. eNeuro 6. https://doi.org/10.1523/ENEURO.0366-18.2019 e0366-18.2019.

Badrinarayan, A., Wescott, S.A., Weele, C.M.V., Saunders, B.T., Couturier, B.E., Maren, S., Aragona, B.J., 2012. Aversive stimuli differentially modulate real-time dopamine transmission dynamics within the nucleus accumbens core and shell. J. Neurosci. 32, 15779–15790. https://doi.org/10.1523/JNEUROSCI.3557-12.2012.

Berghe, N. Van D., Cool, R.H., Horn, G., Wittinghofer, A., 1997. Biochemical characterization of C3G: an exchange factor that discriminates between Rap1 and Rap2 and is not inhibited by Rap1A(S17N). Oncogene 15, 845–850. https://doi.org/10.1038/sj.onc.1201407.

Borsook, D., Becerra, L., Carlezon, W.A., Shaw, M., Renshaw, P., Elman, I., Levine, J., 2007. Reward-aversion circuitry in analgesia and pain: implications for psychiatric disorders. Eur. J. Pain 11, 7–20. https://doi.org/10.1016/j.ejpain.2005.12.005.

Bromberg-Martin, E.S., Matsumoto, M., Hikosaka, O., 2010. Dopamine in motivational control: rewarding, aversive, and alerting. Neuron 68, 815–834. https://doi.org/10.1016/J.Neuron.2010.11.022.

Cepeda, C., Buchwald, N.A., Levine, M.S., 1993. Neuromodulatory actions of dopamine in the neostriatum are dependent upon the excitatory amino acid receptor subtypes activated. Proc. Natl. Acad. Sci. U.S.A. 90, 9576–9580. https://doi.org/10.1073/pnas.90.20.9576.

Clegg, C.H., Correll, L.A., Cadd, G.G., McKnight, G.S., 1987. Inhibition of intracellular cAMP-dependent protein kinase using mutant genes of the regulatory type I subunit. J. Biol. Chem. 262, 13111–13119.

Cohen, J.Y., Haesler, S., Vong, L., Lowell, B.B., Uchida, N., 2012. Neuron-type-specific signals for reward and punishment in the ventral tegmental area. Nature 482, 85–88. https://www.jbc.org/content/262/27/13111.full.pdf.

Correll, L.A., Woodford, T.A., Corbin, J.D., Mellon, P.L., McKnight, G.S., 1989. Functional characterization of cAMP-binding mutations in type I protein kinase. J. Biol. Chem. 264, 16672–16678. https://www.jbc.org/content/264/28/16672.full.pdf.

Danjo, T., Yoshimi, K., Funabiki, K., Yawata, S., Nakanishi, S., 2014. Aversive behavior induced by optogenetic inactivation of ventral tegmental area dopamine neurons is mediated by dopamine D2 receptors in the nucleus accumbens. Proc. Natl. Acad. Sci. U.S.A. 111, 6455–6460. https://doi.org/10.1073/pnas.1404323111.

de Jong, J.W., Afjei, S.A., Pollak Dorocic, I., Peck, J.R., Liu, C., Kim, C.K., Tian, L., Deisseroth, K., Lammel, S., 2019. A neural circuit mechanism for encoding aversive stimuli in the mesolimbic dopamine system. Neuron 101, 133–151. https://doi.org/10.1016/j.neuron.2018.11.005.

Drago, F., Leo, F.D., Giardina, L., 1999. Prenatal stress induces body weight deficit and behavioural alterations in rats: the effect of diazepam. Eur. Neuropsychopharmacol 9, 239–245. https://doi.org/10.1016/s0924-977x(98)00032-7.

Dunwiddie, T.V., Masino, S.A., 2001. The role and regulation of adenosine in the central nervous system. Annu. Rev. Neurosci. 24, 31–55. https://doi.org/10.1146/annurev.neuro.24.1.31.

Elman, I., Upadhyay, J., Langleben, D.D., Albanese, M., Becerra, L., Borsook, D., 2018. Reward and aversion processing in patients with post-traumatic stress disorder: functional neuroimaging with visual and thermal stimuli. Transl. Psychiatry 8. https://doi.org/10.1038/s41398-018-0292-6.

Ferguson, S.M., Eskenazi, D., Ishikawa, M., Wanat, M.J., Phillips, P.E.M., Dong, Y., Roth, B.L., Neumaier, J.F., 2011. Transient neuronal inhibition reveals opposing roles of indirect and direct pathways in sensitization. Nat. Neurosci. 14, 22–24. https://doi.org/10.1038/nn.2703.

Fink, J.S., Weaver, D.R., Rivkees, S.A., Peterfreund, R.A., Pollack, A.E., Adler, E.M., Reppert, S.M., 1992. Molecular cloning of the rat A2 adenosine receptor: selective co-expression with D2 dopamine receptors in rat striatum. Mol. Brain Res. 14, 186–195. https://doi.org/10.1016/0169-328x(92)90173-9.

Franco, R., Navarro, G., 2018. Adenosine A2A receptor antagonists in neurodegenerative diseases: huge potential and huge challenges. Front. Psychiatr. 9, 1–5. https://doi.org/10.3389/fpsyt.2018.00068.

Funahashi, Y., Ariza, A., Emi, R., Xu, Y., Shan, W., Suzuki, K., Kozawa, S., Kozawa, S., Ahammad, R.U., Wu, M., Takano, T., Yura, Y., Kuroda, K., Nagai, T., Amano, M., Yamada, K., Kaibuchi, K., 2019. Phosphorylation of Npas4 by MAPK regulates reward-related gene expression and behaviors. Cell Rep. 29, 3235–3252. https://doi.org/10.1016/j.celrep.2019.10.116.

Hamann, S.B., Ely, T.D., Grafton, S.T., Kilts, C.D., 1999. Amygdala activity related to enhanced memory for pleasant and aversive stimuli. Nat. Neurosci. 2, 289–293. https://doi.org/10.1038/6404.

Harris, C.R., Pashler, H., 2005. Enhanced memory for negatively emotionally charged pictures without selective rumination. Emotion 5, 191–199. https://doi.org/10.1037/1528-3542.5.2.191.

Hoscheidt, S.M., LaBar, K.S., Ryan, L., Jacobs, W.J., Nadel, L., 2014. Encoding negative events under stress: high subjective arousal is related to accurate emotional memory despite misinformation exposure. Neurobiol. Learn. Mem. 112, 237–247. https://doi.org/10.1016/j.nlm.2013.09.008.

Hu, H., 2016. Reward and aversion. Annu. Rev. Neurosci. 39, 297–324. https://doi.org/10.1146/annurev-neuro-070815-014106.

Imai, T., Suzuki, M., SakanoH, 2006. Odorant receptor-derived cAMP signaling direct axonal targeting. Science 314, 657–661. https://doi.org/10.1126/science.1131794.

Jhou, T.C., Fields, H.L., Baxter, M.G., Saper, C.B., Holland, P.C., 2009. The rostromedial tegmental nucleus (RMTg), a major GABAergic afferent to midbrain dopamine neurons, selectively encodes aversive stimuli and promotes behavioral inhibition. Neuron 61, 786–800. https://doi.org/10.1016/j.neuron.2009.02.001.

Klawonn, A.M., Malenka, R.C., 2018. Nucleus accumbens modulation in reward and aversion. Cold Spring Harbor Symp. Quant. Biol. 83, 119–129. https://doi.org/10.1101/sqb.2018.83.037457.

Klawonn, A.M., Fritz, M., Nilsson, A., Bonaventura, J., Shionoya, K., Mirrasekhian, E., Karlsson, U., Jaarola, M., Granseth, B., Blomqvist, A., Michaelides, M., Engblom, D., 2018. Motivational valence is determined by striatal melanocortin 4 receptors. J. Clin. Invest. 128, 3160–3170. https://doi.org/10.1172/JCI97854.

Kravitz, A.V., Tye, L.D., Kreitzer, A.C., 2012. Distinct roles for direct and indirect pathway striatal neurons in reinforcement. Nat. Neurosci. 15, 816–818. https://doi.org/10.1038/nn.3100.

Lobo, M.K., Zaman, S., Damez-Werno, D.M., Koo, J.W., Bagot, R.C., DiNieri, J.A., NugentA, Finkel, E., Chaudhury, D., Chandra, R., Riberio, E., Rabkin, J., Mouzon, E., Cachope, R., Cheer, J.F., Han, M.H., Dietz, D.M., Self, D.W., Hurd, Y.L., Vialou, V., Nestler, E.J., 2013. ΔFosB induction in striatal medium spiny neuron subtypes in response to chronic pharmacological, emotional, and optogenetic stimuli. J. Neurosci. 33, 18381–18395. https://doi.org/10.1523/JNEUROSCI.1875-13.2013.

Maldve, R.E., Zhang, T.A., Ferrani-Kile, K., Schreiber, S.S., Lippmann, M.J., Snyder, G.L., Fienberg, A.A., Leslie, S.W., Gonales, R.A., Morrisett, R.A., 2002. DARPP-32 and regulation of the ethanol sensitivity of NMDA receptors in the nucleus accumbens. Nat. Neurosci. 5, 641–648. https://doi.org/10.1038/nn877.

Matsumoto, M., Hikosaka, O., 2009. Two types of dopamine neuron distinctly convey positive and negative motivational signals. Nature 459, 837–841. https://doi.org/10.1038/nature08028.

McAvoy, T., Zhou, M.M., Greengard, P., Nairn, A.C., 2009. Phosphorylation of Rap1GAP, a striatally enriched protein, by protein kinase a controls Rap1 activity and dendritic spine morphology. Proc. Natl. Acad. Sci. U.S.A. 106, 3531–3536. https://doi.org/10.1073/pnas.0813263106.

McCutcheon, J.E., Ebner, S.R., Loriaux, A.L., Roitman, M.F., 2012. Encoding of aversion by dopamine and the nucleus accumbens. Front. Neurosci. 6, 1–10. https://doi.org/10.3389/fnins.2012.00137.

Meyer, F., Louilot, A., 2014. Consequences at adulthood of transient inactivation of the parahippocampal and prefrontal regions during early development: new insights from a disconnection animal model for schizophrenia. Front. Behav. Neurosci. 7, 1–18. https://doi.org/10.3389/fnbeh.2014.00118.

Mirenowicz, J., Schultz, W., 1996. Preferential activation of midbrain dopamine neurons by appetitive rather than aversive stimuli. Nature 379, 449–451. https://doi.org/10.1038/379449a0.

Nagai, T., Nakamuta, S., Kuroda, K., Nakauchi, S., Nishioka, T., Takano, T., Zhang, X., Tsuboi, D., Funahashi, Y., Nakano, T., Yoshimoto, J., Kobayashi, K., Uchigashima, M., Watanabe, M., Miura, M., Nishi, A., Kobayashi, K., Yamada, K., Amano, M., Kaibuchi, K., 2016a. Phosphoproteomics of the dopamine pathway enables discovery of Rap1 activation as a reward signal in vivo. Neuron 89, 550–565. https://doi.org/10.1016/j.neuron.2015.12.019.

Nagai, T., Yoshimoto, J., Kannon, T., Kuroda, K., Kaibuchi, K., 2016b. Phosphorylation signals in striatal medium spiny neurons. Trends Pharmacol. Sci. 37, 858–871. https://doi.org/10.1016/j.tips.2016.07.003.

Nagel, J., Hauber, W., 2002. Effects of salient environmental stimuli on extracellular adenosinelevels in the rat nucleus accumbens measured by in vivo microdialysis. Behav. Brain Res. 134, 485–492. https://doi.org/10.1016/S0166-4328(02)00062-1.

Nair, A.G., Gutierrez-Arenas, O., Eriksson, O., Vincent, P., Hellgren, K.J., 2015. Sensing positive versus negative reward signals through adenylyl cyclase-coupled GPCRs in direct and indirect pathway striatal medium spiny neurons. J. Neurosci. 35, 14017–14030. https://doi.org/10.1523/JNEUROSCI.0730-15.2015.

Nakanishi, S., Hikida, T., Yawata, S., 2014. Distinct dopaminergic control of the direct and indirect pathways in reward-based and avoidance learning behaviors. Neuroscience 282, 49–59. https://doi.org/10.1016/j.neuroscience.2014.04.026.

O'Neill, C.E., Letendre, M.L., Bachtell, R.K., 2012. Adenosine A_{2A} receptors in the nucleus accumbens bi-directionally alter cocaine seeking in rats. Neuropsychopharmacology 37, 1245–1256. https://doi.org/10.1038/npp.2011.312.

Ögren, S.O., Stiedl, O., 2010. Passive avoidance. In: Stolerman, I.P. (Ed.), Encyclopedia of Psychopharmacology. Springer, Berlin, Heidelberg, pp. 1–10. https://doi.org/10.1007/978-3-540-68706-1_160.

Orellana, S.A., Mcknight, S.G., 1992. Mutations in the catalytic subunit of cAMP-dependent protein kinase result in unregulated biological activity. Proc. Natl. Acad. Sci. U.S.A. 89, 4726–4730. https://doi.org/10.1073/pnas.89.10.4726.

Pan, B.X., Vautier, F., Ito, W., Bolshakov, V.Y., Morozov, A., 2008. Enhanced cortico-amygdala efficacy and suppressed fear in absence of Rap1. J. Neurosci. 28, 2089–2098. https://doi.org/10.1523/JNEUROSCI.5156-07.2008.

Reedquist, K.A., Ross, E., Koop, E.A., Wolthuis, R.M.F., Zwartkruis, F.J.T., Kooyk, Y.V., Salmon, M., Buckley, C.D., Bos, J.L., 2000. The small GTPase, Rap1, mediates CD31-induced integrin adhesion. J. Cell Biol. 148, 1151–1158. https://doi.org/10.1083/jcb.148.6.1151.

Reinstein, J., Schlichting, I., Frech, M., Goody, R.S., Wittinghofer, A., 1991. p21 with a phenylalanine 28 to leucine mutation reacts normally with the GTPase activating protein GAP but nevertheless has transforming properties. J. Biol. Chem. 266, 17700–17706.

Saifullah, M.A., Bin, Nagai, T., Kuroda, K., Wulaer, B., Nabeshima, T., Kaibuchi, K., Yamada, K., 2018. Cell type-specific activation of mitogen-activated protein kinase in D1 receptor-expressing neurons of the nucleus accumbens potentiates stimulus-reward learning in mice. Sci. Rep. 8, 1–12. https://doi.org/10.1038/s41598-018-32840-1.

Sánchez-Catalán, M., Faivre, F., Yalcin, I., Muller, M., Massotte, D., Majchrzak, M., Barrot, M., 2017. Response of the tail of the ventral tegmental area to aversive stimuli. Neuropsychopharmacology 42, 638–648. https://doi.org/10.1038/npp.2016.139.

Scofield, M.D., Heinsbroek, J.A., Gipson, C.D., Kupchik, Y.M., Spencer, S., Smith, A.C., Roberts-Wolfe, D., Kalivas, P.W., 2016. The nucleus accumbens: mechanisms of addiction across drug classes reflect the importance of glutamate homeostasis. Pharmacol. Rev. 68, 816–871. https://doi.org/10.1124/pr.116.012484.

Scott, D.B., Blanpied, T.A., Swanson, G.T., Zhang, C., Ehlers, M.D., 2001. An NMDA receptor ER retention signal regulated by phosphorylation and alternative splicing. J. Neurosci. 21, 3063–3072. https://doi.org/10.1523/JNEUROSCI.21-09-03063.2001.

Shalin, S.C., Zirrgiebel, U., Honsa, K.J., Julien, J., Miller, F.D., Kaplan, D.R., Sweatt, J.D., 2004. Neuronal MEK is important for normal fear conditioning in mice. J. Neurosci. Res. 75, 760–770. https://doi.org/10.1002/jnr.20052.

Smith, R.J., Lobo, M.K., Spencer, S., Kalivas, P.W., 2013. Cocaine-induced adaptations in D1 and D2 accumbens projection neurons (a dichotomy not necessarily synonymous with direct and indirect pathways). Curr. Opin. Neurobiol. 23, 546–552. https://doi.org/10.1016/j.conb.2013.01.026.

Sooksawate, T., Isa, K., Matsui, R., Kato, S., Kinoshita, M., Kobayashi, K., Watanabe, D., Kobayashi, K., Isa, T., 2013. Viral vector-mediated selective and reversible blockade of the pathway for visual orienting in mice. Front. Neural Circ. 7, 1–11. https://doi.org/10.3389/fncir.2013.00162.

Stockwell, J., Jakova, E., Cayabyab, F.S., 2017. Adenosine A1 and A2A receptors in the brain: current research and their role in neurodegeneration. Molecules 22, 1–18. https://doi.org/10.3390/molecules22040676.

Stornetta, R.L., Zhu, J.J., 2011. Ras and Rap signaling in synaptic plasticity and mental disorders. Neuroscientist 17, 54–78. https://doi.org/10.1177/1073858410365562.

Surmeier, D.J., Bargas, J., Hemmings, H.C., Nairn, A.C., Greengard, P., 1995. Modulation of calcium currents by a D1 dopaminergic protein kinase/phosphatase cascade in rat neostriatal neurons. Neuron 14, 385–397. https://doi.org/10.1016/0896-6273(95)90294-5.

Surmeier, D.J., Ding, J., Day, M., Wang, Z., Shen, W., 2007. D1 and D2 dopamine-receptor modulation of striatal glutamatergic signaling in striatal medium spiny neurons. Trends Neurosci. 30, 228–235. https://doi.org/10.1016/j.tins.2007.03.008.

Svenningsson, P., Le, Moine C., Fisone, G., Fredholm, B.B., 1999. Distribution, biochemistry and function of striatal adenosine A_{2A} receptors. Prog. Neurobiol. 59, 355–396. https://doi.org/10.1016/S0301-0082(99)00011-8.

Ungless, M.A., Magill, P.J., Bolam, J.P., 2004. Uniform inhibition of dopamine neurons in the ventral tegmental area by aversive stimuli. Science 303, 2040–2042. https://doi.org/10.1126/science.1093360.

Waltereit, R., Weller, M., 2003. Signaling from cAMP/PKA to MAPK and synaptic plasticity. Mol. Neurobiol. 27, 99–106. https://doi.org/10.1385/MN:27:1:99.

Yamada, K., Tanaka, T., Han, D., Senzaki, K., Kameyama, T., Nabeshima, T., 1999. Protective effects of idebenone and α-tocopherol on β-amyloid-(1-42)-induced learning and memory deficits in rats: implication of oxidative stress in β-amyloid-induced neurotoxicity in vivo. Eur. J. Neurosci. 11, 83–90. https://doi.org/10.1046/j.1460-9568.1999.00408.x.

Yamaguchi, T., Goto, A., Nakahara, I., Yawata, S., Hikida, T., Matsuda, M., Funabiki, K., Nakanishi, S., 2015. Role of PKA signaling in D2 receptor-expressing neurons in the core of the nucleus accumbens in aversive learning. Proc. Natl. Acad. Sci. U.S.A. 112, 11383–11388. https://doi.org/10.1073/pnas.1514731112.

Yang, H., de Jong, J.W., Tak, Y., Peck, J., Bateup, H.S., Lammel, S., 2018. Nucleus accumbens subnuclei regulate motivated behavior via direct inhibition and disinhibition of VTA dopamine subpopulations. Neuron 97, 434–449. https://doi.org/10.1016/j.neuron.2017.12.022.

Zhang, X., Nagai, T., Uddin, R., Kuroda, K., Nakamuta, S., Nakano, T., Yukinawa, N., Funahashi, Y., Yamahashi, Y., Amano, M., Yoshimoto, J., Yamada, K., Kaibuchi, K., 2019. Balance between dopamine and adenosine signals regulates the PKA/Rap1 pathway in striatal medium spiny neurons. Neurochem. Int. 122, 8–18. https://doi.org/10.1016/j.neuint.2018.10.008.

Zhu, Y., Wienecke, C.F.R., Nachtrab, G., Chen, X., 2016. A thalamic input to the nucleus accumbens mediates opiate dependence. Nature 530, 219–222. https://doi.org/10.1038/nature16954.